8 Railway Vehicle Derailment and Prevention

Huimin Wu and Nicholas Wilson

CONTENTS

I. INTRODUCTION

Railway vehicle derailment can cause significant casualties and property loss. Avoidance of derailment is vital to railways for both safety and economic reasons.

Railway vehicle derailments are the results of wheels running off the rails which provide the support and guidance. The reason for wheels running off rails can be very complicated. However, the final scenario of derailment can result in wheels climbing off the rail, rail gauge widening, or rail rollover that causes wheels to fall between rails. Therefore, any conditions that may reduce the lateral guidance provided by rail can increase the risk of derailment.

Note that the derailments discussed in this chapter relate only to the cause of losing lateral constraint at wheel and rail interface. Derailments due to other causes, such as component failure, are not covered in this chapter.

II. HISTORY AND STATISTICS

Derailment has always been one of the major concerns for railway operations since the first day of wheels running on rails. The essential feature of wheels running on rails creates a unique challenge for railways to ensure that wheels stay on the rail. The high speed operation developed in the past century demands a more strict control of vehicle lateral guidance.

Railway technologies have advanced significantly in recent years and safety levels are high compared with the early days and also compared with other transport modes. Derailments however, unfortunately, still frequently occur. Typing "railway derailment" into an internet search, produces pages of derailment incidences around the world, due to different kinds of causes. A very old report can be found that describes the derailment on November 10, 1881 at Carnforth, U.K.[1] This derailment resulted in four passengers being injured, three carriages damaged, and some track damage, and was concluded to be due to the signalman having shifted the facing-points before the entire train had passed over them.

Recently, nearly 40 people were killed when a packed express train crashed in northwestern Turkey on its way from Istanbul to Ankara. It was not immediately clear what had caused the train to derail, but survivors described feeling the carriage violently shaking before the crash.[2]

Railroads in the United States began reporting accidents to the federal government following the passage of the Report Act of 1910.[3] A database of accident/incident has been established since then. Derived from this database, Figure 8.1 displays the North American Freight Railways safety trends between 1980 and 2002.[4] Note that the values for 1980 are taken as a reference defined as 100%. Compared with 1980, a significant reduction in loss and damage has been achieved. However, the trend has been stable since 1992.

According to the FRA accident/incident database, the leading train accident causes are[5]:

- Rail, joint bar, and anchoring
- Track geometry defect
- General switching rules
- Wheels
- Axles and journal bearings

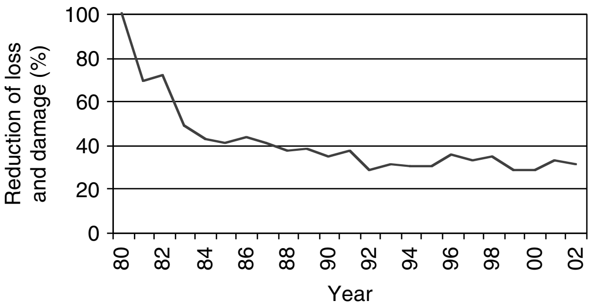

FIGURE 8.1 Loss and damage trends between 1980 and 2000. U.S. (FRA, Railroad Safety Statistics Annual Report 2002).

- Switches
- Frogs, switches and track appliances
- Bogie components
- Train handling/train makeup
- Highway rail grading

In a study of derailments caused by hollow wheels,[6] this database revealed that 8862 reportable derailment incidents occurred between 1998 and 2000. From a review of over 300 derailment incidence cause codes defined by the Federal Railroad Administration (FRA), 53 cause codes were identified as being likely to be influenced by poor wheel–rail interactions.

By further searching the derailment database, 1796 derailments were found relevant to these 53 cause codes between 1998 and 2000. Table 8.1 shows the distribution of the 1796 incidents.

Wide gauge, track alignment, bogie hunting, and wheels with worn tread and flanges were given special attention as they relate directly to poor wheel–rail interaction and are likely to be influenced by hollow-worn wheels. As indicated in Table 8.1, these four cause types are responsible for about 50% of derailments related to the 53 incidence cause codes. Noticeably, wide gauge was reported as the cause of approximately 8% of total reported derailments and approximately 40% of derailments related to the 53 selected cause codes.

Among a large number of derailments, many were caused by mechanical failures of either tracks or vehicles. Some of these failures might be caused by poor designs and others were possibly the accumulative results of undesired performance or poor maintenance.

TABLE 8.1
Distribution of the Researched Incidents

Year	Total Reportable Incidents	Incidents (53 codes)	Wide Gauge	Track Alignment	Hunting	Worn Tread and Flange	Others
2000	3193	673	295	46	7	13	312
1999	2924	612	234	52	6	18	302
1998	2745	511	189	54	3	6	259
Sum	8872	1796	718	152	16	37	873

III. RAILWAY VEHICLE DERAILMENT MECHANISMS AND SAFETY CRITERIA

Railway derailments due to loss of the lateral guidance at the wheel and rail interface may be classified into four major causes: wheel flange climb, gauge widening, rail rollover, and track panel shift, based on the ways that wheel–rail lateral constraints are lost.

A derailment review by Blader discussed the mechanism of these types of derailment and some related test methods.[7]

A. Flange Climb Derailment

Wheel flange climb derailments are caused by wheels climbing onto the top of the railhead then further running over the rail. Wheel climb derailments generally occur in situations where the wheel experiences a high lateral force combined with circumstances where the vertical force is reduced on the flanging wheel. The high lateral force is usually induced by a large wheelset angle-of-attack. The vertical force on the flanging wheel can be reduced significantly on bogies having poor vertical wheel load equalisation, such as when negotiating rough track, large track twist, or when the car is experiencing roll resonances. The forces between the wheel and the rail are explained in more detail in Chapter 4.

Flange climb derailments generally occur on curves. The wheels on the outer rail usually experience a base level of lateral force to vertical force ratio (L/V) that is mainly related to:

- Curve radius
- Wheel–rail profiles
- Bogie suspension characteristics
- Vehicle speed

These factors combine to generate a base wheelset angle of attack, which in turn generates the base level of lateral curving force.

A significantly misaligned bogie is likely to induce higher wheelset angle of attack. Furthermore, any track irregularities and dynamic discontinuities may lead to an additional increase of the wheel L/V ratio. When this ratio exceeds the limit that the wheel can sustain, flange climb occurs.

Wheel climb derailments can also occur on tangent track when track irregularities and vehicle lateral dynamic motion are severe, such as during vehicle hunting and aggressive braking.

1. Wheel Climb Process

The lateral velocity of a wheel due to its rotational velocity is given by

$$V_t = -\omega r \sin(\psi) \tag{8.1}$$

where V_t is the lateral velocity of a wheelset, r is rolling radius, and ψ is wheelset angle of attack.

Figure 8.2 shows a plan view of a wheelset with a yaw angle relative to the track. This angle, which is known more commonly as the angle of attack, contributes to the lateral creepage through a component of the wheelset's rotational velocity.

If the wheelset has a lateral velocity in addition to the component of lateral velocity due to its rotation, the net lateral velocity of the wheelset at the contact zone, assuming the angle of attack to be small, ($\psi = \sin\psi$), is given by,

$$V_y = \dot{y} - \omega r \psi \tag{8.2}$$

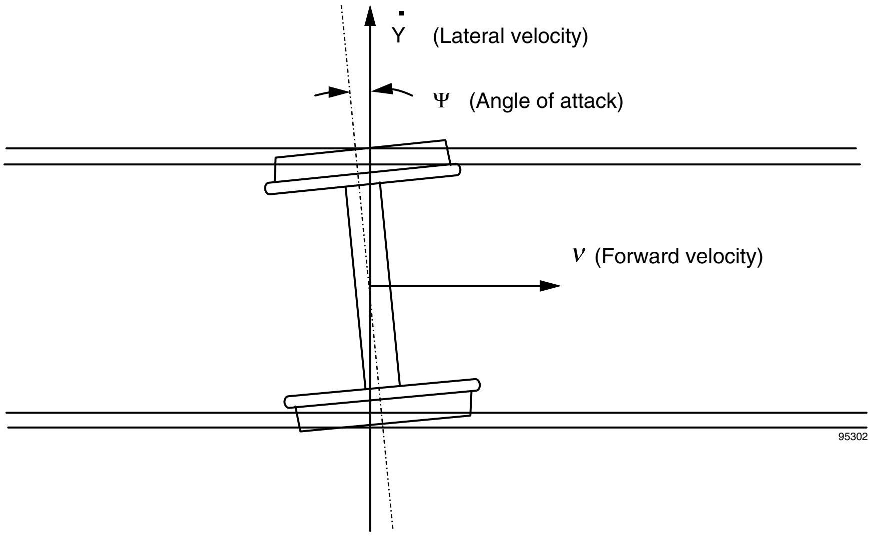

FIGURE 8.2 Wheelset angle of attack.

The lateral creepage is defined as the wheel–rail relative lateral velocity divided by the forward velocity.

$$\gamma_y = \left(\psi - \frac{\dot{y}}{V}\right)\sec(\delta) \tag{8.3}$$

The term $(\psi - \dot{y}/V)$ is commonly known as the effective angle of attack and is a function of the wheelset lateral velocity. It is clear that if the wheelset is moving towards flange contact with a positive angle of attack, the lateral velocity tends to reduce the effective angle of attack.

Since the term $\sec(\delta)$ always has a positive value during flange climb, the direction of the lateral creepage is dependent on the sign of the term $(\psi - \dot{y}/V)$. The lateral creepage equals zero when ψ equals $\dot{y}/V$. The lateral creepage changes direction when $\psi < \dot{y}/V$. The spin creepage also affects the lateral creep force. The direction of the lateral creep force depends on the resultant of the contribution of both the lateral and spin creepages.

The process of the wheel flange climbing up the gauge face and onto the head of the rail may be illustrated in three phases, as Figure 8.3 shows. A single point of contact is assumed in this description.

In phase 1, under the influence of a lateral force, the wheel moves to right towards flange contact. This produces a lateral creep force, acting on the wheel, which is opposing flange climb. In phase 2, as the flange contact angle increases, the wheelset lateral velocity decreases. As a result,

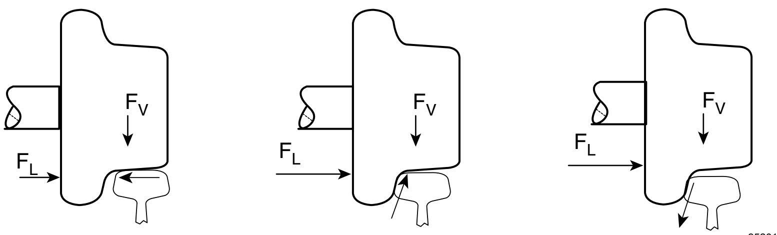

FIGURE 8.3 Process of derailment.

the lateral creepage and creep force reverse direction due to the change in sign of the effective angle of attack. During this phase, the lateral creep force is assisting the wheel to climb. After the maximum contact angle has been passed, the wheelset lateral velocity increases and the wheelset lateral displacement increases rapidly. As a result of the changing wheelset lateral velocity, the effective angle of attack approaches zero and then changes sign. Consequently, the lateral creepage and creep force also reverse direction and, once again, the lateral creep force opposes the climbing motion of the wheel, as shown in phase 3.

2. Flange Climb Safety Criteria

Wheel flange climb derailment phenomena have been investigated for more than 100 years. Several flange climb safety criteria have been proposed. These criteria have been used by railway engineers (globally or locally) as guidelines for safety certification testing of railway vehicles. The following are examples of published criteria:

1. Nadal single-wheel L/V limit criterion
2. Weinstock axle-sum L/V limit criterion
3. High speed passenger distance limit (5 ft) — FRA, U.S.
4. CHXI 50-millisecond time limit — Association of American Railroads, U.S.
5. L/V time duration criterion — proposed by Japanese National Railways (JNR)
6. L/V time duration criterion — proposed by Electromotive Division of General Motors (EMD)
7. Wheel climb distance criterion — proposed by Transportation Technology Centre, Inc. (TTCI)

Criteria 1 and 2 are related to the L/V ratio limits. The rest are related to the time or distance limits, which are applied to limit the exceeding duration of the L/V ratio limit, in either time or distance scale. The wheel climb would be very likely to occur as both the L/V ratio criterion and duration limit are exceeded. There follows a brief description for each criterion listed above.

a. *Nadal Single-Wheel L/V Limit Criterion*

The Nadal single-wheel L/V limit criterion, proposed by Nadal for the French railways, has been used throughout the railway community.[8] Nadal established the original formulation for limiting the L/V ratio in order to minimise the risk of derailment. Nadal assumed that the wheel was initially in two-point contact with the flange point leading the tread point. He concluded that the wheel material at flange contact point was moving downwards relative to the rail material, due to the wheel rolling about the tread contact. He further theorised that wheel climb occurs when the downward motion ceases with the friction saturated at the contact point. Based on Nadal's assumption and a simple equilibrium of the forces between a wheel and rail at the single point of flange contact, as illustrated in Figure 8.4, Equation 8.4 can be derived.

$$
\begin{gathered}
F_3 = V\cos\delta + L\sin\delta = V\left(\cos\delta + \frac{L}{V}\sin\delta\right) \\
\left\{\begin{array}{ll}
F_2 = V\sin\delta - L\cos\delta = V\left(\sin\delta - \frac{L}{V}\cos\delta\right) & \text{when } (V\sin\delta - L\cos\delta) < \mu \times F_3 \\
F_2 = \mu \times F_3 & \text{when } (V\sin\delta - L\cos\delta) \geq \mu \times F_3
\end{array}\right\}
\end{gathered}
\tag{8.4}
$$

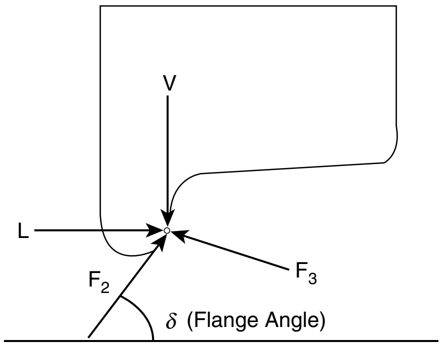

FIGURE 8.4 Forces at flange contact location.

From Equation 8.4, the L/V ratio can be expressed as

$$\frac{L}{V} = \frac{\tan\delta - \dfrac{F_2}{F_3}}{1 + \dfrac{F_2}{F_3}\tan\delta} \tag{8.5}$$

Nadal's famous L/V ratio limiting criterion, given by Equation 8.5, was proposed for the saturated condition $F_2/F_3 = \mu$.

$$\frac{L}{V} = \frac{\tan\delta - \mu}{1 + \mu\tan\delta} \tag{8.6}$$

If the maximum contact angle is used, this equation gives the minimum wheel L/V ratio at which flange climb derailment may occur, for the given contact angle and friction coefficient μ. In other words, below this L/V value, flange climb cannot occur.

Figure 8.5 plots Equation 8.6 for the coefficient of friction range between 0.1 and 1.0.

It indicates that the larger the maximum contact angle, the higher the L/V ratio limit required for flange climb. Figure 8.5 also indicates for the same contact angle, the lower of friction coefficient, the higher the L/V ratio limit required for flange climb.

To explain the effect of wheelset angle of attack (defined in Figure 8.2) on wheel L/V ratio limit, Figure 8.6 displays an example of a single-axle wheel climbing. These are the results from simulations using NUCARS™ (TTCI's rail vehicle dynamic simulation software) and flange climb tests conducted using the Association of American Railroads Track-Loading Vehicle.[9] The wheels used in this example have a flange angle of 75°. In this example, wheel climb will not occur for an L/V ratio level below the solid line for a specified angle of attack. Figure 8.6 also indicates that for large wheelset angles of attack (about 10 mrad in Figure 8.6), derailments occurred at Nadal's value. However, for smaller and negative angles of attack, the L/V ratio required for derailment increased considerably.

In summary, Nadal's criterion agrees with situations when a large angle of attack is experienced, and is conservative for small angles of attack. It does not consider the effects of friction coefficient of the nonflanging wheel on the flanging wheel climbing, which will be discussed in a later section. It assumes flange-climbing derailment is instantaneous once the L/V limit has been exceeded. Both field tests and simulations have proved that wheel flange climb derailments would only occur when the L/V ratio limit has been exceeded for a certain distance limit or time duration limit.

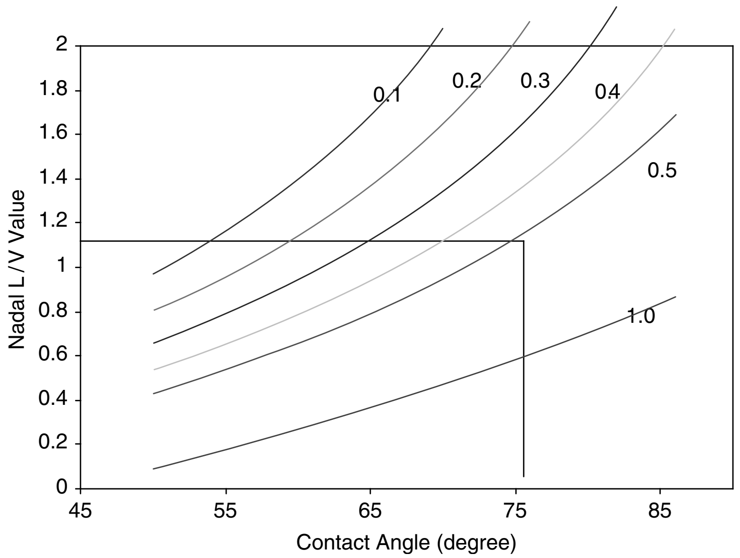

FIGURE 8.5 Relationship of limiting wheel L/V ratio and maximum wheel–rail contact angle. The friction coefficients showed a range of 0.1 to 1.0.

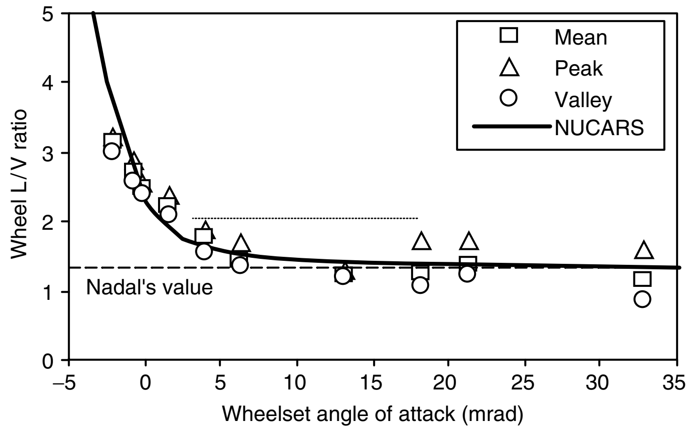

FIGURE 8.6 Effect of wheelset angle of attack on wheel L/V ratio limit.

b. Weinstock Criterion

In 1984, Weinstock proposed a less conservative wheel flange climb criterion.[10] This criterion predicts incipient derailment by summing the absolute values of L/V on the two wheels on the same axle, known as the "axle sum L/V" ratio. The L/V ratio on the flanging wheel is evaluated using the Nadal equation, and the L/V ratio on the nonflanging wheel is generally used to represent the friction coefficient at wheel–rail interface since the nonflanging wheel contacts the rail at wheel tread-rail crown region with a low contact angle (0 to 3° in general).

Weinstock suggested that sum of Nadal value on the flanging wheel and the coefficient of friction on the non-flanging wheel might provide a more accurate criterion than Nadal criterion, especially at small or negative angle-of-attack because Nadal criterion only considered the flange wheel L/V ratio along.

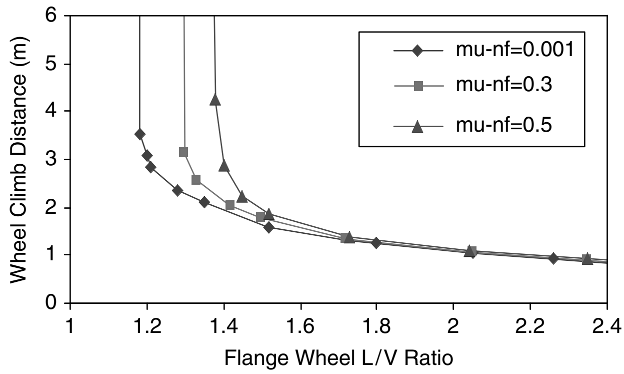

FIGURE 8.7 Effect of nonflanging wheel friction coefficient (5 mrad wheelset angle of attack, 75° flange angle).

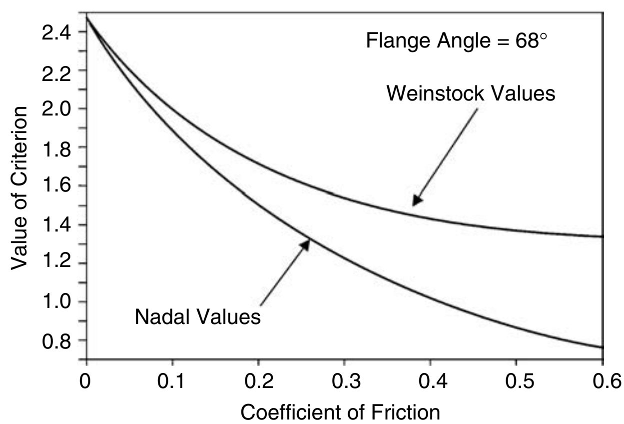

FIGURE 8.8 Comparison of Nadal and Weinstock criteria.[7]

Note that if the coefficient of friction on the nonflange wheel approaches zero, the Weinstock criterion converges with that of Nadal since there is no contribution of L/V value from the nonflange wheel. A flange climb derailment study conducted by Wu and Elkins[11,12] showed that the L/V ratio limit for the flanging wheel increases with the increase of friction coefficient on the nonflange wheel (Figure 8.7). In Figure 8.7, wheel climb will not occur for an L/V ratio level less than the asymptotic line for each friction coefficient level on the nonflanging wheel.

The Weinstock criterion retains the advantage of simplicity. It can be measured with an instrumented wheelset, which measures the values of L/V ratio on both wheels on an axle. It is not only more accurate than Nadal's criterion, it also has the merit of being less sensitive to errors or variations in the coefficient of friction. Figure 8.8 compares the Nadal and Weinstock criteria variation with the coefficient of friction at the wheel–rail interface.

c. Duration Based Criterion

While investigating the duration of the single wheel L/V criterion necessary for derailment, researchers at the JNR proposed a modification to Nadal's criterion.[13] They suggested that for a duration of lateral thrust (lateral force impulse) less than 50 msec, such as might be expected during

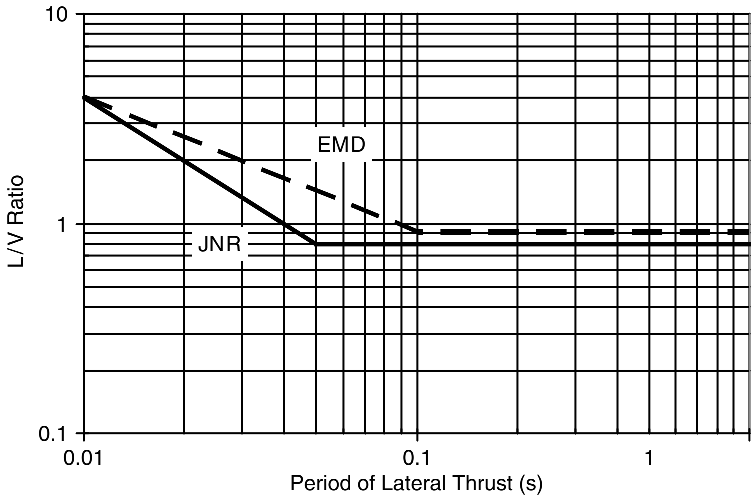

FIGURE 8.9 JNR and EMD flange climb duration criteria.

flange impacts while hunting, the allowable value of the L/V criterion should be increased, as shown in Figure 8.9. The analytical expression for the JNR criterion is given as Equation 8.7. An even less conservative approach was proposed by the Electromotive Division of General Motors (EMD).[14] Its L/V criterion is also shown in Figure 8.9.

$$\frac{L}{V} = \pi\left\{\frac{i_{\mathrm{B}}}{G}\right\}\left\{\frac{\tan(\delta) - \mu}{1 + \mu\tan(\delta)}\right\}\sqrt{\frac{hP_{\mathrm{w}}}{gP}}\left\{\frac{1}{T}\right\} \tag{8.7}$$

d. AAR Wheel Climb Duration Limit (U.S.)

Based on the JNR and EMD research, and considerable experience in on-track testing of freight vehicles, a 0.05 second (50 msec) time duration was adopted by the AAR for the Chapter XI certification testing of new freight vehicles.[15] The Chapter XI criterion states that: "The individual wheel L/V should not exceed 1.0 on any wheels measured. The instantaneous sum of absolute wheel L/V's on any axle shall not exceed 1.5." "(Those values) not to exceed indicated value for a period greater that 50 msec per exceedence."

This time duration has since been widely adopted by test engineers throughout North America for both freight and passenger vehicles that have adopted wheel flange angle of 75°.

e. FRA Wheel Climb Distance Limit (U.S.)

A flange climb distance limit of 5 ft was adopted by the FRA, U.S. for the class 6 (and higher) high speed track standards.[16] This distance limit appears to have been based partly on the results of the joint AAR/FRA flange climb research conducted by TTCI[11] and also on experience gained during the testing of various commuter rail and passenger vehicles.

f. Proposed TTCI Wheel Climb Distance Criterion

The TTCI flange climb criterion was developed for North American freight cars using AAR1B wheel profile with a 75° flange angle at speeds below 80 km/h in curving.[11,12] This criterion encompasses two limits, the single wheel L/V limit and the L/V distance limit. The distance limit is

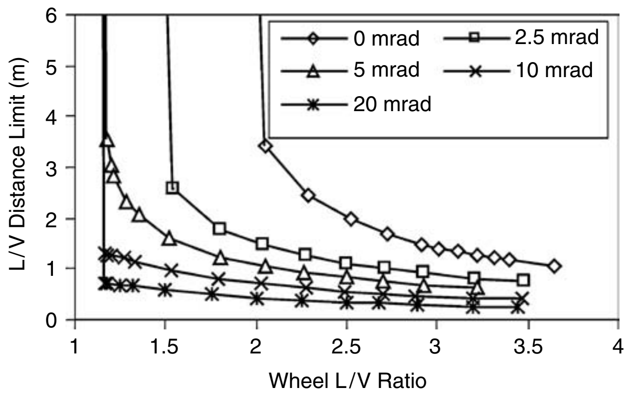

FIGURE 8.10 Effect of wheelset angle of attack on L/V distance limit, $\mu = 0.5$, no longitudinal creepage.

the maximum distance that the single wheel L/V limit can be exceeded without risk of flange climb derailment. It is possibly the first time that the wheelset angle of attack has explicitly been included in the flange climb criterion. Figure 8.10 shows the simulation results of the L/V distance limits under different wheelset angle of attack. The test and simulation results showed that the distance limit is a function of wheelset angle of attack.

The following are the proposed criteria. Since measurements of angle of attack are usually difficult in track test, the criterion is given in two forms: one for the use of simulations in terms of wheelset angle of attack, and one for the use of track test in terms of track curvature (in degrees). Figure 8.11 and Figure 8.12 graphically display the criteria as a function of angle of attack.

Note that both the wheel L/V ratio limit and distance limit will converge to a constant value as the wheelset angle of attack reaches a certain level.

TTCI is currently conducting research to update the proposed criterion and further develop flange climb derailment L/V ratio and distance criteria for application to the North American Freight Railroads and North American Transit Operation. The new criteria will have a more general form for application to the variety of wheel profile designs used by different freight vehicles and transit systems.[17,18] Specific criteria will be specified for the AAR Chapter XI acceptance tests, and for selected transit systems.

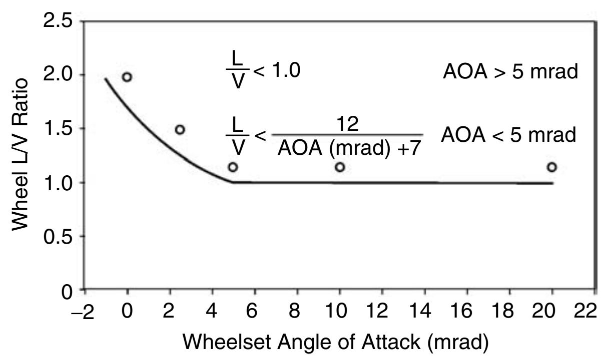

FIGURE 8.11 Proposed single wheel L/V criterion as a function of angle of attack.

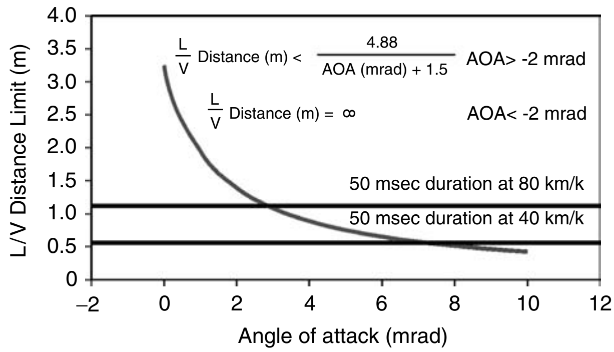

FIGURE 8.12 Proposed L/V distance limit as a function of angle of attack.

B. Application of Flange Climb Derailment Criteria

1. Flange Climb due to Low Flange Angle

Figure 8.13 provides two examples of wheel flange angles. One is a wheel profile with a flange angle of 75° and the other has a 63° flange angle. Referring to Figure 8.5, at a friction coefficient of 0.5, which represents the dry wheel–rail contact condition, the limiting L/V value is 1.13 for wheels with a 75° flange angle, according to the Nadal criterion, and 0.73 for wheels with a 63° flange angle. Clearly, wheels with low flange angles have a higher risk of flange climb derailment.

For historic reasons, some railway systems have adopted relatively low wheel flange angles in the range of 63 to 65°. New systems now generally start with a wheel profile having a flange angle of 72 to 75°.

A wheel profile with a higher flange angle can reduce the risk of flange climb derailment and can have much better compatibility with any new designs of vehicle/bogie that may be introduced compared to wheels with lower flange angles. Also, with a higher L/V ratio limit, high flange angles will tolerate greater levels of unexpected track irregularity.

In the *Track Design Hand Book for Light Rail Transit*,[19] a wheel flange angle of 70° was proposed, based on Professor Heumann's design. *APTA Passenger Rail Safety Standard Task Force Technical Bulletin*[20] provided guidance on reducing the probability of wheel climb derailment by suggesting a minimum wheel flange angle of 72° (suggested tolerances are + 3 and − 2°).

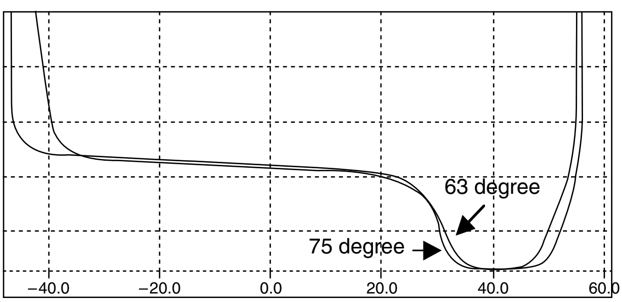

FIGURE 8.13 Wheels with 75 and 63° flange angle.

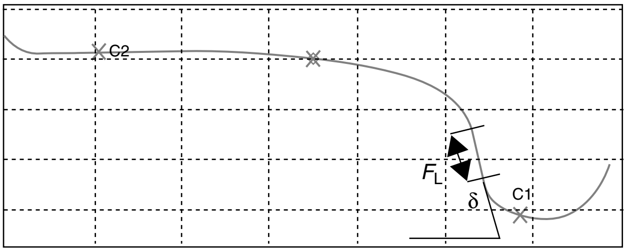

FIGURE 8.14 Definition of flange length.

2. Increase of Flange Length Can Increase Flange Climb Distance Limit

The flange length is defined as a measure of wheel flange contour with an angle above a given degree, explained in Figure 8.14. The flange angle may not be a constant in the length F_L, but must be above a specified value.

A concept of increasing flange length to increase the flange climb distance limit was proposed by Wu and Elkins[11] and further validated by Wilson et al.[21] They concluded that increasing flange length would increase flange climb distance appreciably at a lower angle of attack (approximately 5 mrad), and produce only a small increase in climb distance at a higher angle of attack.

3. Flange Climb due to High Coefficient of Friction at Wheel–Rail Interface

Flange climb derailments have been reported to occur at curves or switches in maintenance yards when the cars were just out of the wheel truing machines. This type of derailment is probably caused by the wheel surface roughness after wheel truing. Figure 8.15 compares a wheel surface just after truing and the surface after many miles of running. The left wheel in Figure 8.15 was trued by the milling type machine with very clear cutting traces on the surface; the middle one was trued by the lathe type machine with shallower cutting traces; and the right wheel was back from operation with a smooth surface but a flat spot on the tread.

Generally, the coefficient of friction for dry and smooth steel-to-steel contact is about 0.5. The effective friction coefficient for the rough surface could be much higher. For example, if the coefficient reaches 1.0, the L/V limit, as shown in Figure 8.5, would be 0.5 for a 75° flange angle and 0.3 for a 63° flange angle. Therefore, the rough surface produced by wheel truing could significantly reduce the L/V limit for flange climb. A low flange angle would further increase the derailment risk. Addressing the final surface tuning and wheel–rail lubrication after reprofiling are two possible remedies to improve the surface condition after reprofiling.

4. Flange Climb of Independently Rotating Wheels

Wheels mounted on a solid axle must rotate at the same speed. To accommodate running in curves, a taper is usually provided on the wheel tread. The wheelset shifts sideways, as shown in Figure 8.16, to allow the outer wheel to run with a larger rolling radius than the inner wheel. The resulting longitudinal creep forces at the wheel–rail interfaces on wheels of the same axle form a moment that steers the bogie around curves (Figure 8.16). Previous flange climb studies have indicated that as the ratio of longitudinal force to vertical force increases, the wheel L/V ratio required for derailment also increases (Figure 8.17). Therefore, the Nadal flange climb criterion can be relaxed based on the level of longitudinal force. The flange climb would occur at an L/V ratio above the Nadal limiting value in the presence of longitudinal force.

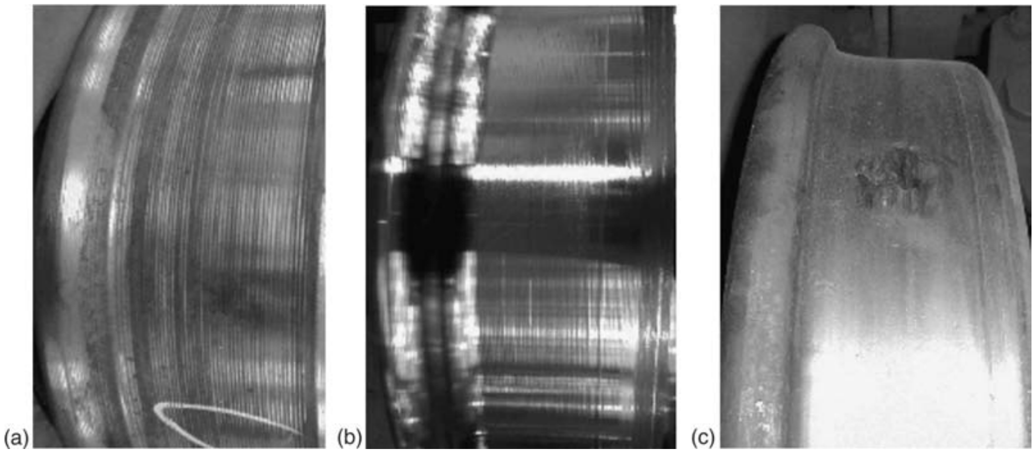

FIGURE 8.15 Comparison of wheel surface roughness. (a) Surface after wheel truing from milling type machine, (b) surface after wheel truing from lathe type machine, (c) surface of wheel back from operation with a flat spot.

In simple terms, the longitudinal steering forces can be viewed as "using up" some of the available wheel–rail friction. This reduces the effective friction coefficient for flange climbing, increasing the L/V ratio required for flange climb.

Independently rotating wheels can rotate at different speeds and therefore produce no longitudinal forces to form a steering moment. This can lead to higher wheelset angles of attack, consequently higher lateral forces (before reaching to the saturation), higher L/V ratios, and increased wheel and rail wear. In addition, since there are no longitudinal forces (the line of $f_{long} = 0$ in Figure 8.17), the wheel–rail friction acts entirely in the lateral direction, resulting in the shortest distance to climb and greater flange climb risk.

In Section III.A.2.a, the conservative nature of the Nadal criterion was discussed. However, for independently rotating wheels, any L/V values that exceed the Nadal limit would cause wheel flange climb because there is no relaxation from the effect of longitudinal force and friction coefficient level on the nonflanging wheel. Therefore, independently rotating wheels have less

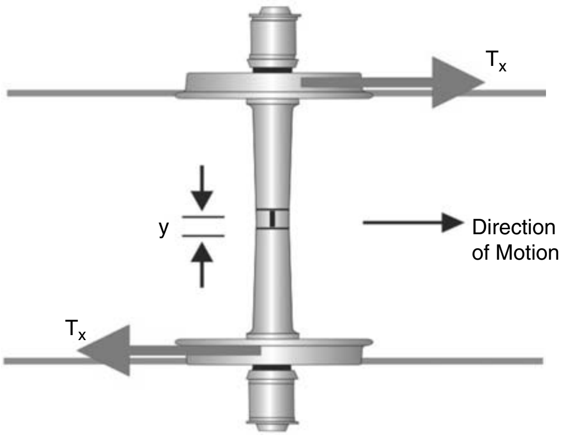

FIGURE 8.16 Steering moment formed by wheel longitudinal forces due to different rolling radius on two wheels.

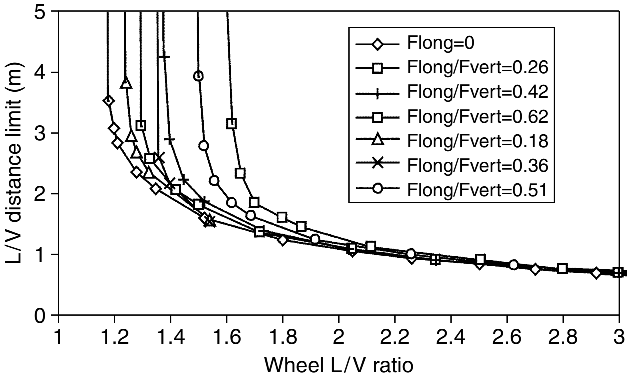

FIGURE 8.17 Effect of wheel L/V ratio on wheel climb distance (5 mrad wheelset angle of attack).[11]

tolerance to track irregularities that may suddenly increase wheel lateral forces or reduce vertical forces.

In summary, vehicles with independently rotating wheels need to be carefully designed to control flange climb and wheel wear. Additional control mechanisms, such as linkages or active control systems, can be used to steer the wheelset on curves and track perturbations. Without such control mechanisms, the wheel–rail profiles, vehicle–track maintenance and wheel–rail friction will need to be much more strictly controlled and monitored to prevent wheel flange climb.

C. Derailments Caused by Gauge Widening and Rail Rollover

Derailments caused by gauge widening usually involve a combination of wide gauges and large lateral rail deflections (rail roll), as shown in Figure 8.18. Large lateral forces from the wheels act to spread the rails in curves. Both rails may experience significant lateral translation and/or railhead roll, which often cause the nonflanging wheel to drop between rails. Figure 8.19 was produced based on a photo of an actual derailment caused by rail rollover, in which the nonflange wheel fell between rails and the outer rail was rolled over. Frequently, the inner rail will rollover due to contact with hollow-worn wheels, as discussed in Section III.C.3.

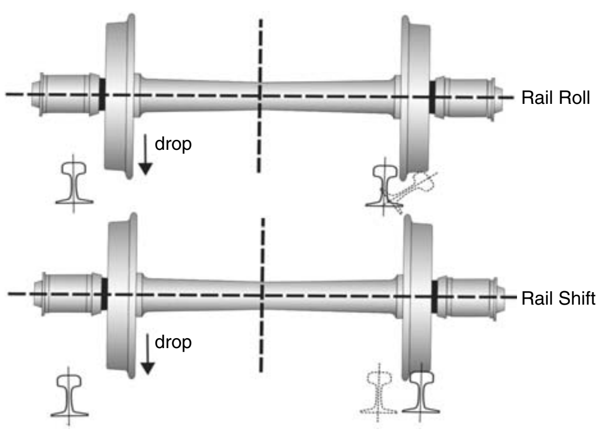

FIGURE 8.18 Gauge widening derailment.[7]

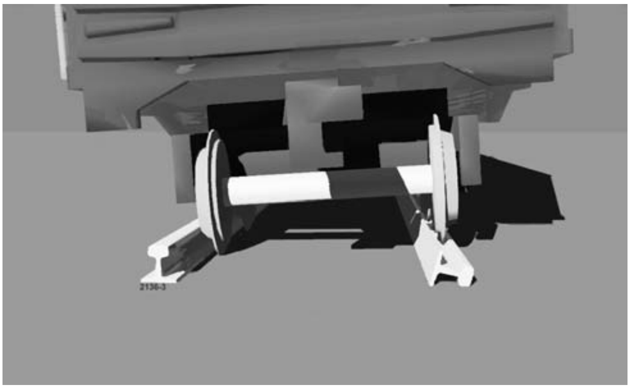

FIGURE 8.19 Nonflange wheel falls between the rails, while the outer rail is rolled over.

When a bogie experiences poor steering, the wheelsets may experience high angles of attack in curves, resulting in large lateral forces exerted on the rails. The poor steering can be caused by inadequate suspensions (generally indicated by low warp or skew stiffness), high bogie turning resistance, misaligned axles, poor wheel and rail profile compatibilities,[22] and wheels having significant tread hollowing. The dynamic forces caused by track lateral perturbations and curve entry/exit spirals can intensify the lateral force level to deflect the rail further.

Locomotives produce high traction forces on rails. Since their bogies are long and can result in large angles of attack, three-axle locomotives (which are now common for heavy haul operation), have been considered as an important cause of gauge widening and rail rollover derailments.

Rail gauge wear is another cause for gauge widening, and is further discussed in Section III.C.2.

1. The AAR Chapter XI Rail Roll Criterion

The AAR Chapter XI rail roll criterion is established by using the L/V force ratio. The rail is assumed to rotate about the rail base corner under the load, as shown in Figure 8.20. The roll moment about the pivot point is given by,

$$M = Vd - Lh \tag{8.8}$$

Under an equilibrium condition, just before the rail starts to roll, M approaches to zero, then,

$$\frac{L}{V} = \frac{d}{h} \tag{8.9}$$

This L/V ratio is considered as the critical value to evaluate the risk of rail roll. When the L/V ratio is larger than the ratio of d/h, the risk of rail roll becomes high.

The critical L/V ratio for rail roll can vary from above 0.6 for contact at the gauge side to approximately 0.2 when the contact position is at the far-field side based on the dimension of rails. This is because the distance d (in Figure 8.20) is reduced. Note that this L/V ratio is calculated assuming that neither the rail fasteners nor the torsional stiffness of the rail section provide any restraint.

When considering the torsional rigidity of rail and the vertical force applied to the rail by the adjacent wheels, a criterion that only considers the forces due to a single wheel may be too conservative for predicting the stability of the rail. Therefore, the limiting criterion has counted the combined forces from all wheels on the same side of the bogie. Hence, a truck (bogie) side L/V ratio

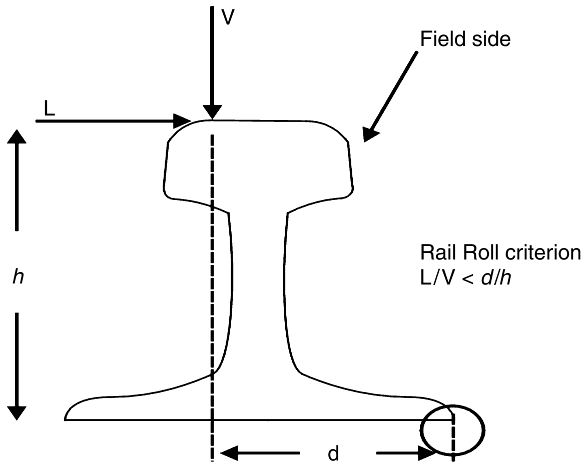

FIGURE 8.20 Illustration of rail roll criterion.

is defined by:

$$\frac{L}{V} = \frac{\text{sum of Lateral forces on truck side}}{\text{sum of Vertical forces on truck side}} \tag{8.10}$$

In Chapter XI of the *Manual of Standards and Recommended Practice* of AAR, the bogie side L/V ratio has been limited to below 0.6 in the vehicle yaw and sway tests.

2. The Gauge Widening Criterion

The gauge widening criterion is related to the wheel and rail geometries and their relative positions, as illustrated in Figure 8.21.

When the wheel drops between the rails, as in Figure 8.18, the geometry of wheel and rail must meet the following expression,

$$G \geq B + W + f_w \tag{8.11}$$

where G, B, W, and f_w are the rail gauge distance, wheel back-to-back space, wheel width, and flange thickness, respectively.

Therefore, a safety margin (S), expressed in Equation 8.12, represents the minimum overlap of wheel and rail required on the nonflanging wheel, when the flanging wheel contacts the gauge face of the rail. In this circumstance, the instantaneous flangeway clearance on the flanging

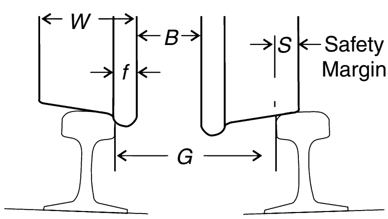

FIGURE 8.21 Wheel and rail geometry related to gauge widening derailment.

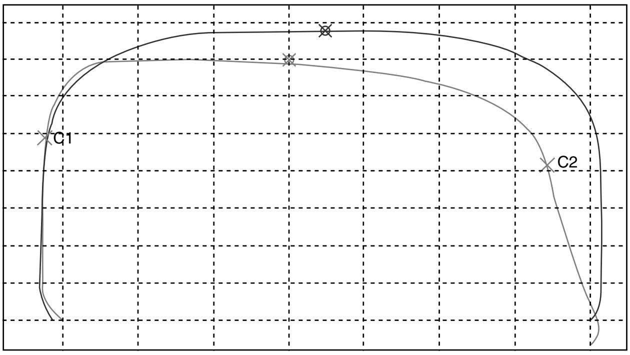

FIGURE 8.22 Gauge widen caused by rail gauge wear.

wheel is zero.

$$(B + W + f_w) - G > S \tag{8.12}$$

In general, the wheel back-to-back space (B) is a constant for a solid axle, and so is the wheel width (W). However, the flange thickness (f_w) is gradually reduced as the wheel wears. The track gauge variations are influenced by multiple factors. As discussed in the previous section, rail roll and the lateral movement of rail due to weakened fasteners can widen the gauge. Rail gauge wear can also contribute to gauge widening, as shown in Figure 8.22, that gives a gauge wear of about 8 mm.

The North American interchange wheel of AAR1B is taken as an example. The back-to-back spacing of the AAR1B is 1350 mm, the wheel width is 145 mm, and the flange thickness is 35 mm. With a standard gauge of 1435 mm, the safety margin is 95 mm. A maximum 31.5-mm gauge widening (include the rail gauge wear measured under an unloaded condition) from the standard value is allowed for a freight vehicle operating in the speed range of 40 to 60 km/h, if a maximum of 15-mm wheel flange wear is allowed. Under this extreme condition, the overlapping is reduced to 48.5 mm. Therefore, any lateral shift and rotation of rail under the loaded condition can further reduce the overlapping to increase the risk of the wheel falling between the rails, especially on poorly maintained track.

3. Effect of Hollow-Worn Wheels on Gauge Widening and Rail Roll Derailment

Wheel hollowing is defined as the vertical difference in rolling radius between the end of the tread and the minimum point around the middle of the tread. The value is found by placing a horizontal line through the highest point on the end of the tread. The wheel tread hollow tends to form a false flange at the end of the tread, as Figure 8.23 illustrates.

Figure 8.24 shows the probable contact condition of a measured hollow-worn wheel on a measured low rail. With wide gauge, or with combined wide rail gauge and thin wheel flange, the false flange of the hollow wheel is likely to contact the top of the low rail towards the field side on curves. Referring to the rail rollover criterion, stated in Equation 8.9, the value of d would be quite low under this condition, leading to a low ratio of d/h. Therefore, any truck (bogie) side L/V ratio larger than this d/h ratio would increase the risk of rail rollover, or put excessive forces on the fasteners. Figure 8.25 shows an example of loose spikes caused by repeated contact towards the field side of the rail.

The contact between the false flange of a hollow wheel and the field side of the inner rail in a curve, can lead to an adverse rolling radius difference condition between the inside wheel and

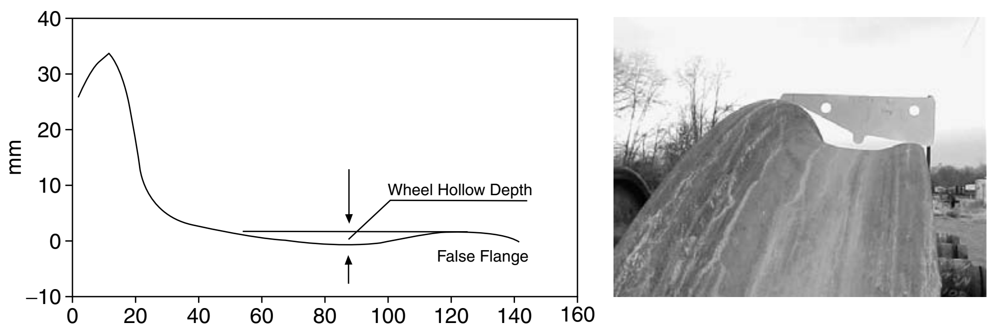

FIGURE 8.23 Hollow-worn wheel.

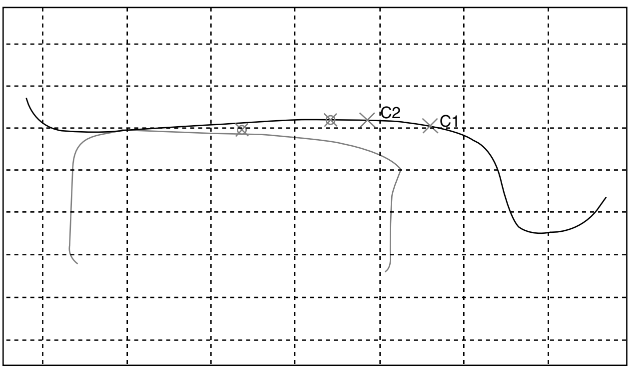

FIGURE 8.24 False flange contact of hollow-worn wheel.

FIGURE 8.25 An example of loose fasteners.

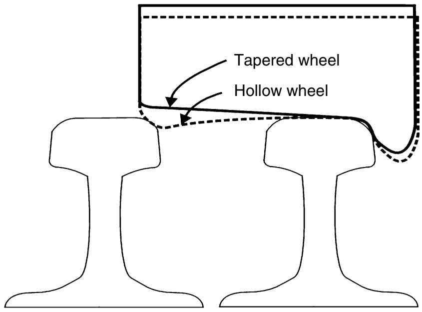

FIGURE 8.26 False flange of a hollow-worn wheel applies a roll force to the stock rail on a riserless switch point.

the outside wheel in curves. Under certain conditions of wheel–rail flange lubrication, this can cause the wheelset steering forces to reverse, increasing the wheelset angles of attack, and lateral forces, causing increased gauge widening and rail rollover.[23]

Switches are consistently among one of the most common track-related causes of derailments. Some incidents of rail rollover derailment in switches are expected to be directly related to hollow wheel profiles. Especially at riserless switch points, a car with hollow-worn wheels may cause rail rollover.[24]

For the vehicle trailing point moves, the wheel stays on the switch point with the false flange hanging down below the level of the stock-rail running surface. As the wheel approaches the point where the two railheads converge, the false flange can strike the side of the stock rail (see Figure 8.26). The high force produced from the false flange–stock rail interaction may either cause a stock rail to roll out, or, in severe cases, a wheel to climb.

D. Derailment Caused by Track Panel Shift

Track panel shift is the cumulative lateral displacement of the track panel, including rails, tie plates and ties, over the ballast, as shown in Figure 8.27. A small shift of these components may not immediately cause the loss of guidance to bogies. However, as the situation gradually depreciates to a certain level, wheels could lose guidance and drop to the ground at some speed. The derailments caused by track panel shift usually result in one wheel falling between the rails and the other falling outside of the track.

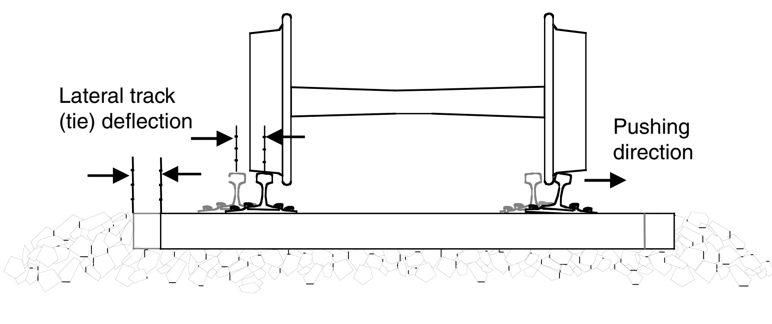

FIGURE 8.27 Lateral track panel shift.

1. Causes of Track Panel Shift

Track panel shift is a lateral misalignment phenomenon primarily caused by repeated lateral axle loads. Tracks that possess low resistance to lateral force, such as poorly laid track, newly laid track, and newly maintained track, often show separations between track panel and ballast. Track panels could shift under large lateral forces under such conditions. The capacity of a track panel to resist lateral movement is measured by lateral track strength and stiffness. Soft subgrade may also allow the panel to shift more freely.

Track panel shift has become increasingly important as both speed and load increase and more continuous welded rail is placed in use. The increase in speed may result in an increase in the unbalanced forces on curves or poorly aligned track by curving considerably above the balance speed. At high imbalance speeds, the wheelsets of many bogie designs stop generating gauge spreading forces, and instead, both wheels generate wheel–rail forces that act to force the rails outwards in a curve, leading to panel shift.

The escallation in load can increase the magnitude of lateral force at the wheel and rail interface. Continuous welded rail may buckle due to the longitudinal force caused by temperature change. Aggressive acceleration and braking can also induce large forces to cause panel shift on track with poor lateral resistance.

Knothe and Bohm[25] commented that how near the BB 9104 locomotive came to a catastrophe when it archived the world record (of 331 km/h in 1955). The test locomotive has caused a strong sinusoidal alignment fault of the track. There seem to have been two causes. The first is probably that the track was tamped just before the record test. By this maintenance operation the strength of track to resist lateral displacements was reduced. The second cause is that the locomotive was unstable, thus exerting high lateral forces on the dislodged ballast bed.

2. Panel Shift Criterion

Lateral track strength indicates the capability of track to resist track buckling and to retain lateral alignment under traffic. Track buckling is defined as the lateral deformation of track due to high compressive rail force in the longitudinal direction at a temperature above the rail neutral temperature. Track panel shift normally accumulates gradually. However, when the critical load level is exceeded, panel shift increases rapidly with the number of repeated load applications.

The definition of the critical lateral load can be based on either accumulated or incremental deformation after each load application. Note that with each load pass, the increment of total deformation (elastic plus residual) remains constant for a stable track. Below critical loads, the elastic deformation remains constant and the residual deformation tends to zero. With each load pass over a segment of unstable track, both elastic and residual deformation increment will grow.

Research by the French National Railways suggested that the limiting lateral axle load can be defined in a general expression (Equation 8.13) for preventing excessive track panel shift,[7,26]

$$L_c = aV + b \tag{8.13}$$

where L_c is the critical lateral load and V is the vertical axle load. Table 8.2 lists two groups of suggested values of a and b.

A further multiplying factor of 0.85 was specified for use in Canada[7] to allow for the quality of tie-down and ties-in in some tracks. Then, Equation 8.13 is reformatted as,

$$L_c = 0.85(aV + b) \tag{8.14}$$

TABLE 8.2
Suggested Values of *a* and *b*

Prud'homme	$a = 0.333$ $b = 9.96$ kN for uncompacted ballast	$a = 0.333$ $b = 14.99$ kN for well compacted ballast and concrete ties
Ahlbeck and Harrison	$a = 0.4$ $b = 9.96$ kN for uncompacted ballast on wood ties	$A = 0.7$ $b = 24.6$ kN for compacted ballast on wood ties

A multiplying factor proposed by Ahlbeck and Harrison considered the effect of track curvature and temperature in determining the lateral force limit.[7]

$$A = 1 - \frac{S\Delta}{22,300}(1 + 0.46D) \tag{8.15}$$

where S is the area of rail section (square inches), Δ is temperature change (degree Fahrenheit) and D is degree of track curvature.

The lateral track strength and track panel shift study conducted by Li and Shust[26] concluded that vertical axle load has a major effect on the resistance of a track panel to lateral deflection. The lateral track strength and stiffness would only be valid for a given vertical load. In their in motion panel shift test, the critical lateral axle force for causing panel shift is approximately 15 to 30% higher for track with concrete ties than wood tie track.

E. Derailment Caused by Vehicle Lateral Instability

On tangent track, the wheelset generally oscillates around the track centre due to any vehicle and track irregularities, as shown in Figure 8.28. This movement occurs because vehicle and track are never absolutely smooth and symmetric. This self-centring capability of a wheelset is induced by the coned shape of the wheel tread. However, as speed is increased, if the wheelset conicity is high, the lateral movement of wheelset, as well as the associated bogie and car body motion, can cause oscillations with large amplitude and a well-defined wavelength. The lateral movements are limited only by the contact of the wheel flanges with the rail. This vehicle dynamic response is also termed as vehicle hunting, and can produce high lateral forces to damage track and to cause derailments.

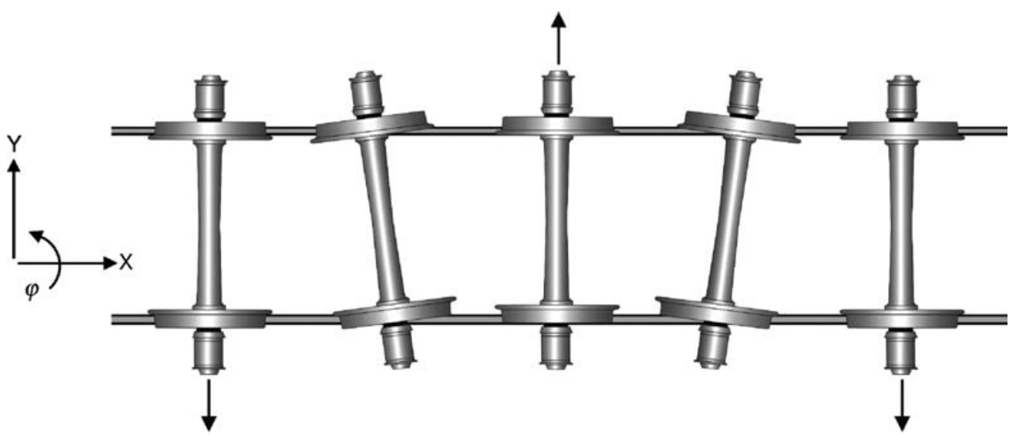

FIGURE 8.28 Wheelset oscillates around the track centre.

Derailments caused by vehicle hunting can have derailment mechanisms of all the four types discussed in the previous sections. The high lateral force induced from hunting may cause wheel flange climbing on the rail, gauge widening, rail rollover, track panel shift, or combinations of these. The safety concerns for this type of derailment, usually occurring at higher speeds, make it an important area of study.

Hunting predominantly occurs in empty or lightweight vehicles. The critical hunting speed is highly dependent on the vehicle/track characteristics. When vehicle hunting is onset, the displacements of wheelset are generally large, alternatively flanging from one side of the rails to the other. Considering the wheel/rail geometry and the creep force saturation, the vehicle/track system under hunting conditions should be treated as nonlinear. Investigation of the critical speed for such a system with nonlinearities is to examine the vehicle dynamic response to a disturbance using a numerical solution of the equations of motion.[27]

Vehicle simulation computer models, which include the processes to solve these equations of motion, are often used to predict the hunting speed. Track tests are also generally required to either validate the hunting speed predicted by modelling or ensure the system operating speed is below the hunting onset speed.

The effective conicity of wheel–rail contact has considerable influence on the vehicle hunting speed. As wheelset conicity increases, the onset critical speed of hunting decreases. For this reason, it is important when designing wheel and rail profiles to ensure that, for a specific bogie/vehicle, the critical hunting speed is above the operating speed.

IV. PREDICTION OF DERAILMENT

Three types of approach are usually used for predicting the risks of derailment or diagnosing the causes of derailments: assessment of wheel/rail parameters, dynamic simulations of vehicle–track interaction and vehicle performance track tests. In many cases, all three approaches are applied.

A. Assessment of Wheel/Rail Parameters

Assessment of wheel/rail parameters may predict the risks of derailment that are the result of unfavourable wheel–rail contact. Since wheel and rail are operating as a mechanical system involving two-body contact and interaction, this assessment of wheel/rail parameters should include wheels operating on the line where rails are measured (or designed for the new line condition). The contact parameters that may affect derailment include:

- Maximum contact angle and length of flange (related to flange climb)
- Rolling radius difference on curves (related to flange climb)
- Effective conicity (related to vehicle lateral instability on tangent track)
- Rail gauge (related to gauge widening)
- Contact positions (related to rail rollover)
- Wheel–rail contact conformity (affects bogie steering and level of lateral forces)
- Rolling radius difference of two wheels on a same axle (affects bogie steering)
- Level of wheel tread hollowing (related to rail rollover, also affects wheel climb and vehicle instability under certain conditions, and rolling radius difference)
- Significant wear of wheel flange and rail gauge can increase wheelset lateral movement and may reduce the effectiveness of restraining rail on curves

A comprehensive view of wheel–rail contact at a system level is important to reveal the overall patterns of the contact. For example, thousands of wheels with different profiles (due to different levels of wear or resulting from different bogie performances) contact a section of rail at different positions and could produce different levels of contact stress. Therefore, the performances of the majority of wheel–rail pairs are of interest in system assessment.

However, derailments are often related to the behaviours of individual wheels and rails that possess undesired shapes. In diagnosing the causes of derailment, the wheel profiles on derailed cars and rail profiles at derailment sections must be measured and analysed to study the contributions from the wheel/rail shapes.

B. Dynamic Simulation of Vehicle–Track Interaction

Since the 1980s, computer simulations have been extensively used to study vehicle–track interaction (see Chapter 12). They are also useful tools to diagnose the causes of derailments. For some derailments, the explicit causes cannot be simply identified. Some derailments cannot even be repeated by track tests that appear to have similar conditions as the derailed cars and tracks. The advantages of a computer modelling study are that parameters of vehicle/track can be conveniently (also cost effectively) varied to investigate the effects of either single parameters or combinations of multiple parameters on derailments. Consequently, if the simulation reveals derailment risk, modifications to vehicle and track for preventing derailments can also be defined by a parametric study.

The flange climb risk can be evaluated in the simulation using the flange climb criteria discussed in Section III.A including the L/V ratio limit and exceeding distance (or time) limit. Simulation of derailments caused by gauge widening and panel shift under dynamic load requires more advanced vehicle/track simulation models that include the capability of rail roll under the load, which results in changing wheel–rail contact condition, and a detailed track model to describe the structure below the rail.

The accuracy of the description of vehicle and track parameters is crucial for simulation to reflect the actual responses of vehicle and track. For example, a sudden change of wheel/rail forces due to large track lateral irregularity combined with wheels with low flange angle could lead to derailment. Therefore, only this irregularity and the shape of the wheels are accurately described in the model with other vehicle/track parameters, the derailment scenario will be reproduced by the simulation. When evaluating a system, it is important to examine the vehicles under the worst track conditions possibly allowed in the system in order to ensure safe operation under those conditions. When examining newly designed (or modified) vehicles, a certain limit of wear of vehicle elements and wheel profiles should also be considered in the simulations.

C. Track Tests

On-track tests are generally required for new designs or modifications of vehicles. Track tests are also often conducted for diagnosing performance problems, including derailment, caused by vehicle or track conditions, or a combination of both. These vehicles may have been examined by computer simulation. However, precisely describing every element and parameter in the vehicle/track system is very difficult, especially for those nonlinear elements, such as friction elements, damping elements, and gaps/stops. Modelling can reveal the trends or probable performances with regard to derailment. Track tests will demonstrate the actual performance under different test conditions for the test unit. Therefore, computer simulations and track tests are often combined efforts in derailment evaluations or diagnoses.

On-track tests of new vehicle designs is required for the North American Freight Service. Chapter XI of the *Manual of Standard and Recommended Practices*, approved by the Association of American Railroads, describes the regimes of vehicle performance to be examined and the required test conditions.[15] The test regimes in Chapter XI include:

- Hunting (vehicle lateral instability)
- Constant curving
- Spiral

- Twist, roll
- Pitch
- Yaw, sway
- Dynamic curving

Usually, the test unit is instrumented with a number of gauges to measure forces, accelerations, and displacements at critical locations on the test unit depending on the test objective. Instrumented wheelsets have been applied in recent years to determine more accurately wheel–rail interaction forces. The wheel L/V ratio limit (or axle L/V ratio limit) and the exceeding distance (or time) limit are used in Chapter XI tests to evaluate vehicle curving performance. Wheel unloading is also an important criterion used in the Chapter XI test. It limits the level of minimum vertical wheel force to no less than 10% of static load.

The FRA (U.S.A.) has also implemented a requirement for testing of new passenger trains that run at speeds above 90 mi/h (144 km/h) for passenger cars and 80 mi/h (128 km/h) for freight cars.[16]

The Railway Safety and Standard Board of the U.K. has issued railway groups standards relevant to engineering acceptance. These standards describe the permissible track forces for railway vehicles.[28,29]

V. PREVENTION OF DERAILMENT

Most derailments may be prevented if the problems, related either to vehicles or tracks, that lead to derailment could be identified and adequate preventive actions could be taken at an early stage.

The four types of derailments discussed in the previous sections have a common cause of high lateral force at the wheel–rail interface. Therefore, any conditions that lead to high lateral forces or lead to lower the ability of the system to sustain the force should be corrected.

In this section, some general preventive methods are introduced. However, due to the wide range of vehicle types and track conditions, any methods that are adopted by a system to prevent derailment must be carefully assessed by considering the specific vehicle and track conditions in that system to ensure the effectiveness of the methods.

A. Wheel/Rail Profiles

1. Addressing Wheel Flange Angle

To prevent flange climb derailment, the maximum wheel flange angle should be sufficiently high to increase the allowed L/V ratio limit. For a new wheel profile design, a higher flange angle should be emphasised. A flange angle above 70° is generally recommended. Should flange climb derailments be a concern to an existing system that has adopted wheels with a low flange angle, a transition to a higher flange angle might be considered. However, this transition needs to be carefully planned according to the capacity of wheel truing and rail grinding in the system.[30]

2. Removing Hollow-Worn Wheels

Removing significantly hollowed worn wheels from the system may reduce the risk of gauge widening and rail rollover derailment, as described in Section III.C.3. Hollow wheels can also reduce rolling radius difference required in curving and increase lateral instability on tangent track.[31,32] A starting 4-mm hollow wheel removing limit has been recommended by TTCI for the North American interchange operation. The aim is to eventually remove the wheels with 3-mm hollow tread from the service.[33]

B. Independently Rotating Wheels

As discussed in Section III.B.3, independently rotating wheels tend to run with a larger angle of attack in curves than the conventional coupled wheelsets and can generate greater lateral forces that increase the risk of wheel climb. Therefore, independent rotating wheels require more carefully designed wheel profiles and control mechanisms for curving. Elkins[34] and Suda et al.[35] have proposed self-steering bogies with independent rotating wheels equipped on the trailing axle only. In recent years, the concept of active control has been studied.[36,37] As the yaw angle and lateral motion of wheels can be accurately controlled, more applications of independent rotating wheels can be expected.

C. Installation of Guard Rail or Restraining Rail on Sharp Curves

Restraining rails and guard rails have been frequently applied in transit operations on sharp curves to prevent flange climb derailment (or to reduce gauge wear on the high rail). The restraining/guard rails are generally installed inside of the low rail, as shown in Figure 8.29. In extremely sharp curves restraining rails are sometimes installed on both the inside and outside rails.

The clearance between the low rail and the restraining rail is critical for the effectiveness of restraining rails. Too tight clearance may reduce wheelset rolling radius difference required for bogie curving by limiting the flange contact on the high rail. Overwide clearance may completely lose the restraining function.

Wear at the wheel flange back and the contact face of the restraining rail can vary the clearance between the low rail and the restraining rail. The wheel flange and high rail gauge wear can affect the amount of wheelset lateral shift on curves. Note that track lateral geometry irregularities, including alignment and gauge variations can also affect the performance of restraining rails.

D. Optimising Bogie Suspension and Bogie Yaw Stiffness

The suspension design of a bogie affects its steering capability. Bogies with soft primary suspensions that allow the axles to steer in curves generally generate lower lateral forces than bogies with stiff primary suspensions. However, if the primary suspension is too soft, high-speed stability may be reduced. Therefore, optimising bogie suspension to meet the specific requirements of a system (mainly in terms of track condition and operating speed) is essential for the bogie design.

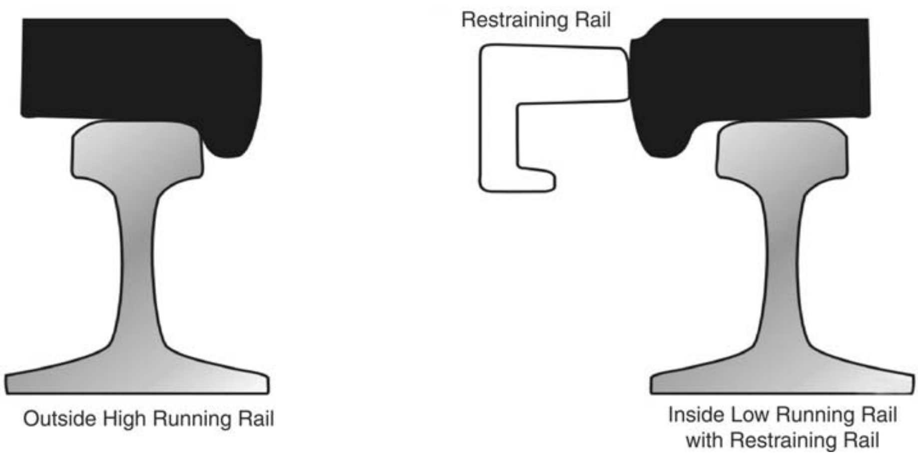

FIGURE 8.29 Restraining rail.

E. LUBRICATION

Friction plays an important role in wheel-rail interface. It affects many wheel–rail interaction scenarios. With respect to derailment, proper lubrication at the wheel–rail interface can reduce wheel lateral forces because wheel lateral creep force (F_{lat}) saturates at a lower level ($F_{\mathrm{lat}} = \mu N$, *N is the contact normal force*). Therefore, the potential of wheel climbing and gauge widening is reduced. As illustrated in Figure 8.4, the limiting wheel L/V ratio for wheel climb increases with the decreases in the friction coefficient at contact surface.

In recent years, top-of-rail friction management, with an intermediate range of coefficient of friction (from 0.2 to 0.4), has been tested.[38,39] Application of top-of-rail friction modifiers is intended to reduce rolling resistance, corrugation, and eliminate wheel squeal. Top-of-rail friction management can also be expected to reduce vehicle lateral instability on tangent track.

F. TRACK GEOMETRY INSPECTION AND MAINTENANCE

Severe track lateral and vertical irregularities and gauge widening are significant causes of derailment. On many railways, track geometry recording cars are used regularly to survey the track. The frequency of survey varies greatly, between monthly and yearly, according to track category.[16,40] Track is categorised based on a combination of maximum speed and annual tonnage. Regular visual inspection is often carried out at much shorter intervals (between once and twice a week). Regulations of track geometry for different regions and railways may be different. However, maintenance is normally required when the track geometry deviations exceed the specified limits.

Note that newly laid or newly maintained track requires special attention due to its low lateral strength. Speed restrictions may be required for a period to let the track settle.

G. SYSTEM MONITORING

Derailments usually occur from a combination of unfavourable vehicle and track conditions. Normally, only a single vehicle with a particular problem derails in a section of track with an adverse condition. On the other hand, a bogie with a particular defect usually does not derail in every section of track. A program of system monitoring can be implemented to detect any derailment-related vehicle and track problems, including wheel/rail profiles, in their early stages. Then, corrective action can be promptly taken to prevent occurrences of derailment.

REFERENCES

1. http://home.clara.net/gw0hqd/bumps/101181/101181.htm (Carnforth derailment)
2. http://news.com.au/common/story_page/0,4057,10221240%255E1702,00.html (Turkey derailment)
3. FRA Guide for Prepare Accident\Incident Report, U.S. Department of Transportation, Federal Railroad Administration, May 2003.
4. Railroad Safety Statistics, Annual Report 2002, U.S. Department of Transportation, Federal Railroad Administration.
5. *Safety Database Analysis*, Transportation Technology Center, Inc., 2002.
6. Harry, T., Wu, H., and Guins, T., *The Influence of Hollow-Worn Wheels on the Incidence and Costs of Derailments*, Association of American Railroads/Transportation Technology Center, Inc. report R-965, February 2004.
7. Blader, F.B., *A Review of Literature and Methodologies in the Study of Derailments Caused by Excessive Forces at the Wheel/Rail Interface*, Association of American Railroads Report R-717, December 1990.
8. Nadal, M.J., *Locomotives a Vapeur*, Collection Encyclopedie Scientifique, Biblioteque de Mecanique Appliquee et Genie, Vol. 186, Paris, 1908.

9. Shust, W.C., Elkins, J.A., Kalay, S., and El-Sibaie, M., *Wheel-Climb Derailment Tests using AAR's Track Loading Vehicle*, Association of American Railroads Report R-910, December 1997.
10. Weinstock, H., *Wheel Climb Derailment Criteria for Evaluation of Rail Vehicle Safety*, Proceedings of ASME Winter Annual Meeting, 84-WA/RT-1, New Orleans, LA, 1984.
11. Wu, H. and Elkins, J., *Investigation of Wheel Flange Climb Derailment Criteria*, Association of American Railroads Report R-931, July 1999.
12. Elkins, J. and Wu, H., *New Criteria for Flange Climb Derailment*, IEEE/ASME Joint Railroad Conference, Newark, NJ, April 4–6, 2000.
13. Matsudaira, T., *Dynamics of High Speed Rolling Stock*, Japanese National Railways RTRI Quarterly Reports, Special Issue, 1963.
14. Koci, H. H. and Swenson, C. A., *Locomotive Wheel-Loading — A System Approach*, General Motors Electromotive Division, LaGrange, IL, February, 1978.
15. M1001, AAR Mechanical Division, *Manual of Standards and Recommended Practices*, Section C — Part II, Volume 1, Chapter XI, Section 11.5.2 Track-Worthiness Criteria, Adopted 1987, Revised 1993.
16. Federal Railroad Administration. *Track Safety Standards*, *Part 213, Subpart G,* September, 1998.
17. Wu, H., Shu, X., and Wilson, N., *Flange Climb Derailment Criteria and Wheel/Rail Profile Management and Maintenance Guidelines for Transit Operations — Appendix B*, Transit Cooperate Research Program Report 71, Vol. 5, 2005.
18. Wilson, N., Shu, X., Wu, H., and Tunna, J., *Distance-Based Flange Climb L/V Criteria*, Association of American Railroads/Transportation Technology Center, Institute of Technology Digest, TD-04-012, July 2004.
19. *Track Design Handbook for Light Rail Transit*, Transit Cooperate Research Program, Report 57, 2000.
20. *Passenger Rail Safety Standard Task Force Technical Bulletin*, 1998-2001, Part 1.
21. Wilson, N., Shu, X., and Kramp, K., *Effect of Independently Rolling Wheels on Flange Climb Derailment*, Proceedings of ASME International Mechanical Engineering Congress, November, 2004.
22. Mace, M., Dibrito, D., Blank, R., Keegan, S., and Michael, Allran, *Effect of Wheel Profiles on Gauge Widening Behaviour*, Proceeding of ASME/IEEE Joint Railroad Conference, March, 1994.
23. Mace, S., Pena, R., Wilson, N., and Dibrito, D., Effect of wheel-rail contact geometry on wheelset steering forces, *Wear*, 191(1–2), January, 1996.
24. Singh, S. and Davis, D.D., *Effect of Switch-Point Risers on Turnout Performance*, Association of American Railroads, Transportation Technology Center, Inc., Technology Digest 98-018, June 1998.
25. Knothe, K. and Bohm, F., History of stability of railway and road vehicles, *Vehicle Syst. Dyn.*, 31(5–6), June, 1999.
26. Li, D. and Shust, W., *Investigation of Lateral Track Strength and Track Panel Shift Using AAR's Track Loading Vehicle*, AAR/TTCI report R-917, December 1997.
27. Wickens, A., *Fundamentals of Rail Vehicle Dynamics — Guidance and Stability*, Swets & Zeitlinger, Lisse, 2003.
28. *Permissible Track Forces for Railway Vehicles*, British Railways Board, GM/TT0088, October 1993.
29. *Commentary on Permissible Track Forces for Railway Vehicles*, Railtrack, UK, 1995.
30. Wu, H., Shu, X., and Wilson, N., *Flange Climb Derailment Criteria and Wheel/Rail Profile Management and Maintenance Guidelines for Transit Operations — Appendix A*, Transit Cooperate Research Program Report 71, Vol. 5, 2005.
31. Sawly, K., Urban, C., and Walker, R., *The Effect of Hollow-Worn Wheels on Vehicle Stability in Straight Track*, Proceedings of Contact Mechanics and Wear of Rail/Wheel System, The Sixth International Conference, June, 2003.
32. Sawley, K. and Wu, H., *The Formation of Hollow-Worn Wheels and Their Effect on Wheel/Rail Interaction*, Proceedings of Contact Mechanics and Wear of Rail/Wheel System, The Sixth International Conference, June, 2003.
33. Sawley, K. and Clark, S., *The Economics of Removing Hollow Wheels from Service*, Association of American Railroads/Transportation Technology Center, Ins. Technology Digest, TD-99-034, December 1999.
34. Elkins, J. A., *Independently Rotating Wheels. A Simple Modification to Improve the Performance of the Conventional Three-Piece Truck*, Proceedings of the Ninth International Wheelset Congress, Montreal, Quebec, Canada, September, 1988.

35. Suda, Y., Nishimura, R., Kata, N., Matsumoto, A., Sata, Y., Ohno, H., Tanimoto, M., and Miyauchi, E., Self-steering tricks using unsymmetrical suspension with independently rotating wheels — Comparison between stand tests and calculations, *Vehicle Syst. Dyn.*, 33, 2000.
36. Mei, T.X. and Goodall, R.M., Wheelset control strategies for a two-axle railway vehicle, *Vehicle Syst. Dyn.*, 33, 2000.
37. Shen, S., Mei, T. X., Goodall, R. M., Pearson, J., and Himmelstein, G., *A Study of Active Steering Strategies for Railway Bogies*, 18th IAVSD Symposium, Dynamics of Vehicles on Road and Tracks, August, 2003.
38. Eadie, D. and Stantoro, M., *Railway Noise and the Effect of Top of Rail Liquid Friction Modifiers: Changes in Sound and Vibration Spectral Distributions*, Proceedings of Contact Mechanics and Wear of Rail/Wheel System, The Sixth International Conference, June, 2003.
39. *Guidelines to Best Practices for Heavy Haul Railway Operations: Wheel and Rail Interface Issues*, International Heavy Haul Association, May 2001.
40. Federal Railroad Administration. *Track Safety Standards*, Part 213, Subpart A to F, September, 1998.